Structure Refinement of $Li_4Mn_5O_{12}$ with Neutron and X-Ray Powder Diffraction Data

Toshimi Takada[1] and Etsuo Akiba

National Institute of Materials and Chemical Research, Higashi 1-1, Tsukuba, Ibaraki 305, Japan

Fujio Izumi

National Institute for Research in Inorganic Materials, Namiki 1-1, Tsukuba, Ibaraki 305, Japan

and

Bryan C. Chakoumakos

Oak Ridge National Laboratory, P.O. Box 2008, Building 7962, Oak Ridge, Tennessee 3783-6393

Well-crystallized $Li_4Mn_5O_{12}$ powder was prepared by heating a eutectic mixture of lithium acetate LiOAc and manganese nitrate $Mn(NO_3)_2$ in an O_2 atmosphere. The structure of $Li_4Mn_5O_{12}$ crystallites was found to be cubic spinel using Rietveld refinement of both neutron and X-ray powder diffraction profiles. We confirmed that lithium ions occupy both the tetrahedral sites 8a and part of the octahedral sites 16d, but not the 16c sites in the space group $Fd\bar{3}m$, while all the manganese ions occupy the 16d sites. The lattice parameter was found to be sensitive to synthesis temperature as a result of the variation in manganese valence. The presence of Mn^{3+} leads to the formation of a stoichiometric spinel $Li[Li_xMn_{2-x}]O_4$ in which x decreases from 1/3 ($Li_4Mn_5O_{12}$) to 0 ($LiMn_2O_4$), with concomitant formation of Li_2MnO_3 depending on the synthesis conditions. © 1997
Academic Press

1. INTRODUCTION

Lithium manganese oxides have been extensively studied as the cathode materials for advanced rechargeable lithium batteries because they offer high cell voltage, good rechargeability, and a wide operating temperature range with a much lower cost compared to $LiNiO_2$ and $LiCoO_2$. Particular attention has been given to the spinels $LiMn_2O_4$ (1–4), $Li_4Mn_5O_{12}$ (5–8), and $Li_2Mn_4O_9$ (9, 10). Currently, the spinel $Li[Li_xMn_{2-x}]O_4$ (0.03 < x < 0.10) is becoming more attractive because it shows better cycling performance. It was found that the onset of the structural changes caused

by the Jahn–Teller distortion upon deep discharging could be suppressed by introducing a small amount of Li ions into the 16d sites to keep the average Mn oxidation state slightly above 3.5 (2, 11). It is the current consensus that a wide range of solid solution exists within the Li–Mn–O family of spinel compounds, and that the composition of the spinel electrode plays a very important role in controlling the rechargeability of the electrode (3). Therefore, attention should be paid to the control of the synthesis process to obtain single-phase samples with the required stoichiometry. Understanding the structural changes during the synthesis process is crucial for both process control and understanding the variation of the voltage, the capacity, and the cycling performance of Li/spinel cells.

Studies on Mn^{4+} defect spinels $Li_2O \cdot yMnO_2$ (y = 2.5–4) with end members $Li_4Mn_5O_{12}$ (y = 2.5) and $Li_2Mn_4O_9$ (y = 4) are, however, limited to those poorly crystallized powders obtained from the solid state reaction of Li_2CO_3 or LiOH, and $MnCO_3$ or MnO_2 at temperatures below 400°C, because the concomitant formation of Mn^{3+} occurs by the reduction of Mn^{4+} when the reaction temperature is raised above 400°C. Recently we reported that well-crystallized $Li_4Mn_5O_{12}$ can be prepared at a temperature up to 700°C from a eutectic mixture by using lithium acetate LiOAc and manganese nitrate $Mn(NO_3)_2$ as starting materials (6, 7). The structure of $Li_4Mn_5O_{12}$ crystallites was previously studied by X-ray powder diffraction. Ideally, $Li_4Mn_5O_{12}$ with all Mn ions in the 4+ oxidation state should be isostructural to the spinel $LiMn_2O_4$ with the cation distribution $(Li)_{8a}[Li_{1/3}Mn_{5/3}]_{16d}O_4$, in which oxygen ions form a cubic-close-packed array occupying 32e sites of the space group $Fd\bar{3}m$; Li ions occupy 8a sites

[1] To whom correspondence should be addressed.

(one-eighth of the tetrahedral sites), and co-occupy 16d sites (half of the octahedral sites) with Mn ions. Experimentally, however, we found the oxidation state of manganese to be somewhat lower than 4.0, since it is very difficult to eliminate the presence of Mn^{3+} in the $Li_4Mn_5O_{12}$ samples, which can be better expressed as $Li_4Mn_5O_{12-\delta}$ ($0 < \delta \leq 0.25$). The distribution of Li ions, which determines the performance of the electrode, is also difficult to determine because Li is a very weak X-ray scatterer.

In this study, we have focused on the confirmation of the cation distribution and structural changes caused by the presence of Mn^{3+}. Since the spinel $Li_4Mn_5O_{12}$ can only be prepared in powder form, the structural information is best obtained using profile refinement methods. Here we use the well-established Rietveld method (12) to analyze both the X-ray and neutron powder diffraction profiles of $Li_4Mn_5O_{12}$ prepared at various temperatures. Our structural results agree with those previously reported, but are more quantitative. The formation of spinel $Li[Li_xMn_{2-x}]O_4$ at elevated temperature is elucidated.

2. EXPERIMENTAL

Synthesis of $Li_4Mn_5O_{12}$. Pure (99.9%) $LiOAc \cdot 2H_2O$ and $Mn(NO_3)_2 \cdot 6H_2O$ (from WAKO Pure Chemical Industries, Ltd.) were used as starting materials. Stoichiometric amounts of the raw materials were first heated at 100°C to obtain a uniform eutectic solution and then slowly oxidized at 200°C under flowing O_2, thereby converting the eutectic solution to a solid Li–Mn–O precursor. Powder samples were obtained by heating the ground precursor at temperatures ranging from 400°C to 900°C for 1–3 days. All samples were heated at a rate of 100°C/hr and slowly cooled to room temperature in the furnace (about 7 hr) with 200 ml/min of flowing O_2. Details of the preparation process are described in our previous report (6). Samples heated at 700°C for 1 day and 500°C for 2 days are designated as 700-1D and 500-2D, respectively.

X-ray diffraction. X-ray powder diffraction measurements were conducted at room temperature on a Rigaku RAX-I X-ray diffractometer with $CuK\alpha$ radiation monochromated by a graphite single crystal at 40 kV, 30 mA. Data were collected between $2\theta = 15°–120°$ with a step interval of 0.03°.

Neutron diffraction. Neutron-diffraction data were collected using the HB4 high-resolution powder diffractometer at the High-Flux Isotope Reactor equipped with a Ge (115) monochromator at Oak Ridge National Laboratory (ORNL). The neutron wavelength was found to be 1.4180(2) Å on the basis of unit cell refinements for a silicon standard. Each sample (4.5 g) was placed in a spinning vanadium can (1 cm i.d. by 6 cm) at 295 K, for data collection over the 2θ range 11°–135° in steps of 0.05°.

The structural refinements were carried out with the Rietveld refinement program RIETAN-94 (13) on a Power Macintosh 8100/100AV. The mean oxidation number of manganese (Z_{Mn}) in the sample was determined from the active oxygen content which was measured by the standard volumetric method (14) of $KMnO_4$ titration.

3. RESULTS AND DISCUSSION

3.1. Structural Refinement of $Li_4Mn_5O_{12}$ by the Rietveld Method

Refinements were initiated in the space group $Fd\bar{3}m$ using the initial structural model with atomic coordinates from our previous X-ray diffraction study of $Li_4Mn_5O_{12}$. The following neutron scattering lengths were used: $b_{Li} = -0.1900 \times 10^{-14}$ m, $b_{Mn} = -0.3730 \times 10^{-14}$ m, $b_O = 0.5803 \times 10^{-14}$ m. The simultaneous refinement was carried out on two crystalline phases: $Li_4Mn_5O_{12}$ (space group $Fd\bar{3}m$, No. 227) and Li_2MnO_3 ($C/2m$, No. 12). The crystallographic parameters of Li_2MnO_3 were adopted from Strobel and Andron (15). Only the scale factor and cell parameters of Li_2MnO_3 were refined because of its small content ($< 5\%$). It was confirmed that the simultaneous refinement improves the "goodness of fit" indicator, S, and results in smaller R factors for both X-ray and neutron profiles. In addition, small diffraction peaks from Li_2MnO_3 as indicated by arrows in Fig. 1 appeared in both neutron and X-ray diffraction profiles. To obtain better consistency between the X-ray and neutron diffraction data, several constraints were imposed in the final refinements. The site occupancy of the octahedrally coordinated manganese ions in the 16d sites was finally refined based on the X-ray diffraction data because manganese is more sensitive to X-ray, while the occupancy of Li in the 8a sites and oxygen in the 32e sites and overall isotropic thermal parameters were determined using the neutron diffraction data. We could not perform the combined X-ray and neutron Rietveld refinement using RIETAN-94. By introducing the constraints to the refinement of X-ray and neutron diffraction profiles separately, and repeating the refinements step by step, we were able to match both the neutron and X-ray powder diffraction patterns with very similar structural parameters. The final observed, calculated, and difference profiles are shown in Fig. 1 and the refined lattice parameter, atomic coordinates, thermal parameters, and interatomic distances for $Li_4Mn_5O_{12}$ (sample 700-1D) are listed in Tables 1 and 2.

The site occupancies confirmed that the ion distribution is very close to the ideal arrangement, $(Li)_{8a}[Li_{1/3}Mn_{5/3}]_{16d}O_4$ (16). The occupation of the interstitial 16c sites by Li and the 8a sites by Mn are ruled out. Allowing variation of the oxygen site occupancy results in a value of 1.0 within the standard deviation, which indicates that the oxygen is very nearly stoichiometric in this sample.
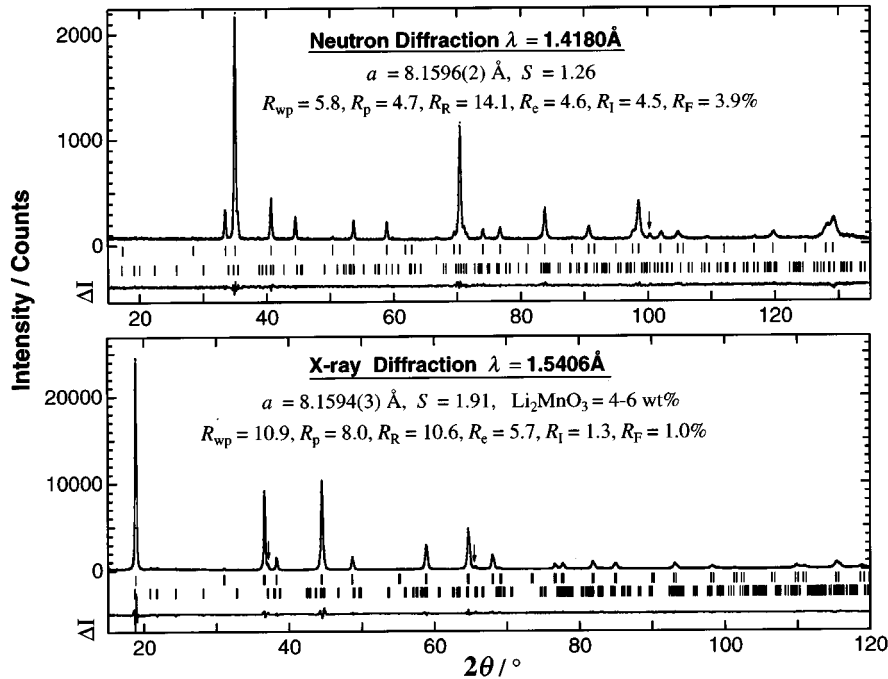
FIG. 1. Rietveld refinement profiles for the $Li_4Mn_5O_{12}$ sample prepared at 700°C. Observed (dots) and calculated (solid line) intensities are shown at the top, and the difference of the observed and calculated intensities (ΔI) are shown at the bottom. The tick marks below the pattern indicate the positions of all possible Bragg reflections from $Li_4Mn_5O_{12}$ (upper) and Li_2MnO_3 (lower). R factors as defined in (12) are given for reference.

Instead, the occupancy of manganese in the 16d sites, g_{Mn}, is found to be 0.84, with an estimated standard deviation (e.s.d.) of 0.02. The value of g_{Mn} is a little higher than, but in good agreement with, the 0.833 value of the ideal arrangement $(Li)_{8a}[Li_{1/3}Mn_{5/3}]_{16d}O_4$, in which 0.333 Li ions are required to compensate for the imbalance in charge in the 16d sites assuming all the manganese ions are in the 4+ state. From the electroneutrality point of view, a higher value of g_{Mn} indicates the presence of Mn^{3+} ions. As a result,

the precipitation of Li_2MnO_3 appears to consume the excess Li ions. The refined lattice parameter and oxygen parameter (the fractional coordinate of oxygen) of $Li_4Mn_5O_{12}$ are 8.1594(3) Å, 0.3878(3), and 8.1596(2) Å, 0.3880(1) from X-ray and neutron diffraction data, respectively. They are identical within the experimental errors. Good consistency in the interatomic distance for $Li_4Mn_5O_{12}$ was also obtained from X-ray and neutron diffraction data as shown in Table 2.

3.2. Structural Changes of $Li_4Mn_5O_{12}$ with Synthesis Temperatures

Analogous refinement of the data for a sample prepared at low temperature resulted in similar crystallographic

TABLE 1
Structural Parameters of $Li_4Mn_5O_{12}$ Prepared from LiOAc and $Mn(NO_3)_2$ at 700°C under Flowing Oxygen

Space group: $Fd\bar{3}m$, No. 227 $a^b = 8.1594(3)$ Å, $a^c = 8.1596(2)$ Å

Atom	Site	$x = y = z$	g	B (Å^2)
Li(1)	8a	0.0	1.00(5)[c]	1.0 (2)[c]
Li(2)[a]	16d	0.625	0.16	$= B(Mn)$
Mn	16d	0.625	0.84(2)[b]	0.40(5)[b]
O	32e	0.3878(3)[b]	1.00(2)[c]	0.80(4)[c]
		0.3880(1)[c]		

Note. All numbers in parentheses present the e.s.d. of the last significant digit, and g is the occupancy.

[a] Constrains on occupancies $g(Mn) + g(Li(2)) = 1$ and isotropic thermal parameters $B(Li(2)) = B(Mn)$ were applied.

[b] Parameters refined using the X-ray diffraction data.

[c] Parameters refined using the neutron diffraction data.

TABLE 2
Interatomic Distances in $Li_4Mn_5O_{12}$ at 295 K

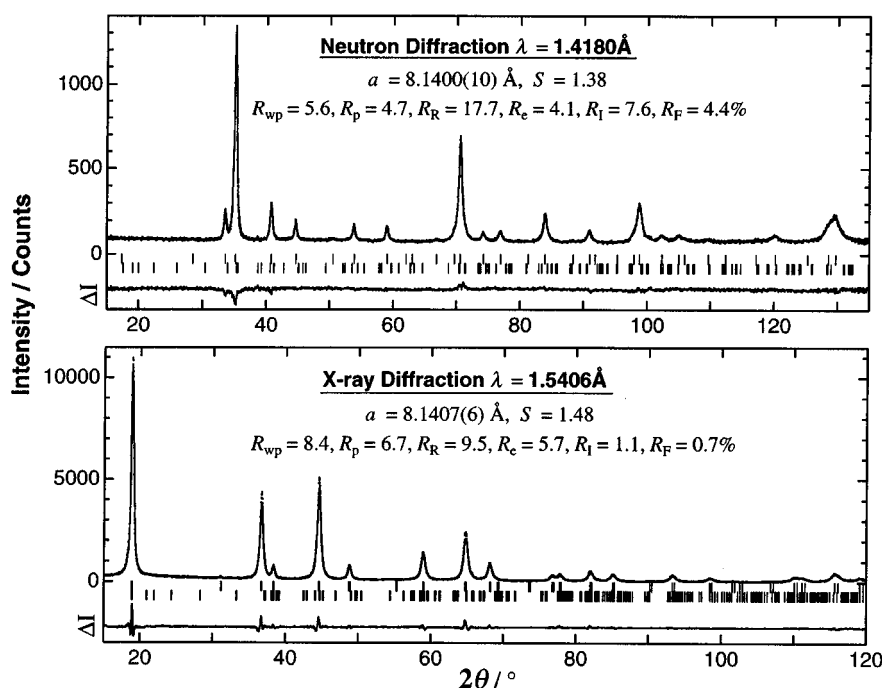| Bond	X-ray	Neutron
Li1–O	$1.9481(47) \times 4$	$1.9506(14) \times 4$
Mn(Li2)–O	$1.9406(24) \times 6$	$1.9395(7) \times 6$
Li1–Mn(Li2)	3.3827(1)	3.3828(1)
Li1–Li1	3.5331(1)	3.5332(1)
Mn–Mn	2.8848(1)	2.8849(1)

Note. Numbers in parentheses are the estimated standard errors.

FIG. 2. Rietveld refinement profiles for the $Li_4Mn_5O_{12}$ sample prepared at 500°C. See legend of Fig. 1 for the descriptions of the data.

parameters. Figure 2 and Table 3 show the Rietveld refinement plot and the structural parameters for the $Li_4Mn_5O_{12}$ sample prepared at 500°C (500-2D). The diffraction peaks were broader than those of the 700-1D sample, therefore overlapping the reflections from the minor phase Li_2MnO_3. The amount of Li_2MnO_3 was found to be less than 2 wt%. The peak intensity of the sample 500-2D was much lower than that of the 700-1D sample, indicating the lower crystallinity of the spinel $Li_4Mn_5O_{12}$. The crystallographic parameters for this sample are almost identical to that of the sample 700-1D, except for the lattice parameter $a = 8.1405(10)$ Å. This indicates about 0.7% contraction in volume of the unit cell from the sample prepared at 700°C. The refined site occupancy of manganese in the 16d sites, g_{Mn}, is 0.83 ± 0.01 which is identical to 0.833 of the ideal arrangement, indicating that the oxidation state of manganese in this sample is very close to 4+.

To better understand the changes in lattice parameter, the bond length of Li–O and Mn–O, and the oxygen parameter, u, with the synthesis temperature, analogous refinements of the X-ray diffraction data for all samples prepared at temperatures in the range 400 to 900°C were performed, and the results are plotted in Fig. 3. For simplicity, the Mn–O bond represents the bond between oxygen and the cations in octahedral sites (Mn and Li ions that occupy 16d sites). The oxygen parameter slightly increased with synthesis temperature from 0.3872(3) to 0.3886(3). These numbers are much larger than the ideal value for spinel structure, 0.375, which implies that Li–O tetrahedra are larger than the Mn–O octahedra. The change in the bond length of Mn–O with synthesis temperature is rather small, whereas the Li–O bond is likely to be more ionic than the Mn–O bond and thus expands more readily with temperature (16, 17).

Refinement of the manganese site occupancy factor revealed that g_{Mn} increased with synthesis temperature. The refined g_{Mn} for spinel Li–Mn–O and the portion of precipitated Li_2MnO_3 in the final products are plotted in Fig. 4
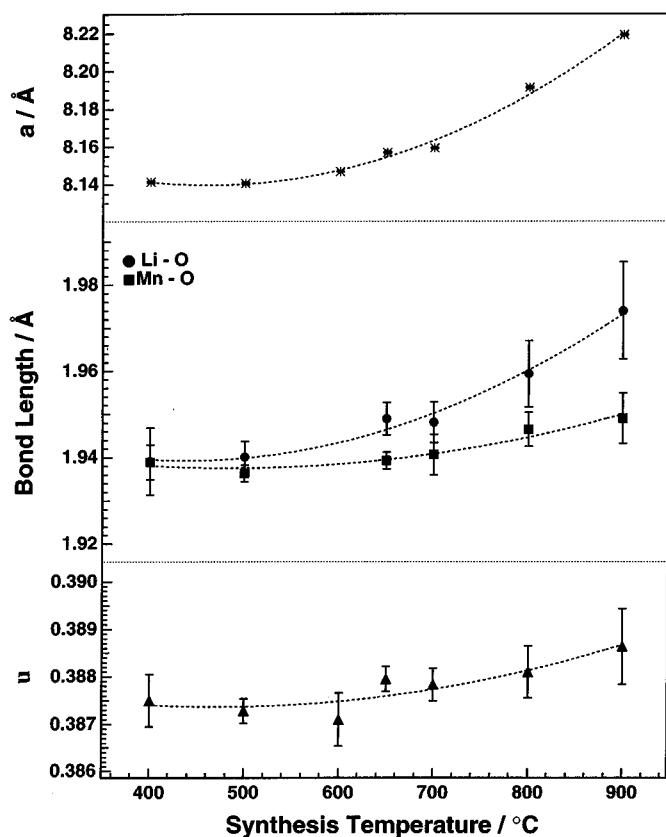
TABLE 3
Structural Parameters of $Li_4Mn_5O_{12}$ Prepared from LiOAc and $Mn(NO_3)_2$ at 500°C under Flowing Oxygen

Space group: $Fd\bar{3}m$, No. 227 $a^b = 8.1407(6)$ Å, $a^c = 8.1400(10)$ Å

Atom	Site	$x = y = z$	g	$B(Å^2)$
Li(1)	8a	0.0	1.0	1.0
Li(2)[a]	16d	0.625	0.17	$= B(Mn)$
Mn	16d	0.625	0.83(1)[b]	0.37(5)[b]
O	32e	0.3873(3)[b] 0.3880(2)[c]	1.0	0.80(5)[c]

Note. All numbers in parentheses present the e.s.d. of the last significant digit, and g is the occupancy.

[a] Constrains on occupancies $g(Mn) + g(Li(2)) = 1$ and isotropic thermal parameters $B(Li(2)) = B(Mn)$ were applied.

[b] Parameters refined using the X-ray diffraction data.

[c] Parameters refined using the neutron diffraction data.

FIG. 3. Changes in bond lengths Li–O and Mn–O and the oxygen parameter u with synthesis temperature, along with the lattice parameter for the spinel Li–Mn–O.

FIG. 4. Plot of the refined g_{Mn}, the portion of precipitated Li_2MnO_3 against the synthesis temperature, along with the lattice parameter of the spinel Li–Mn–O.

against the synthesis temperature, along with the lattice parameter. As synthesis temperature was raised to 900°C, the site occupancy g_{Mn} reached 1.0, which indicates a change in the composition of the spinel phase. Since no evidence for oxygen deficiency in the $32e$ sites was found in these refinements, the spinel phase should be stoichiometric with a composition, lying on the tie line between $Li_4Mn_5O_{12}$ and $LiMn_2O_4$ in the Li–Mn–O diagram (2, 3), which can be simply expressed as $Li_{1+x}Mn_{2-x}O_4$ ($1/3 \leq x \leq 0$). In this case, the increase in g_{Mn} from 0.83 to 1.0 corresponds to a composition transition of the spinel phase from $Li_4Mn_5O_{12}$ to $LiMn_2O_4$, whereby the manganese oxidation state decreases from 4.0 to 3.5, and the molar ratio of Li/Mn in the spinel phase decreases from 0.8 to 0.5. The increase in the lattice parameter with synthesis temperature, therefore, can be easily ascribed to the presence of larger Mn^{3+} ions in the samples prepared at elevated temperatures. The effective ion radii of octahedrally coordinated Mn^{3+} and Mn^{4+} are 0.645 (in high-spin state) and 0.56 Å, respectively (18). The precipitation of Li_2MnO_3, thus, occurs to consume the excess Li.
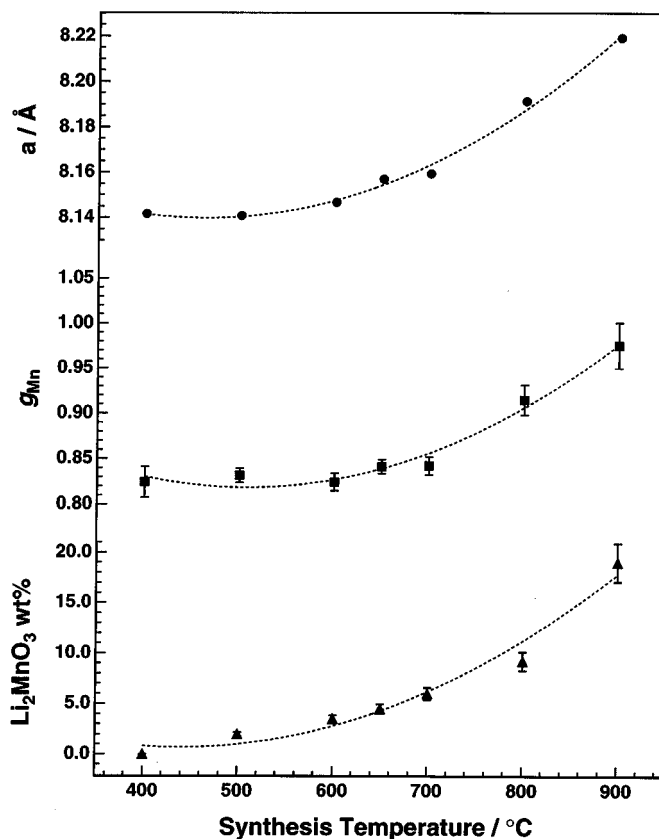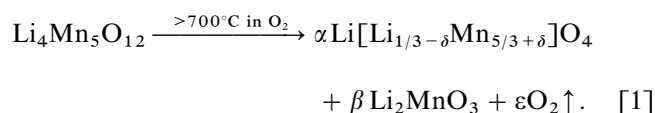
The composition transition of the spinel from $Li_4Mn_5O_{12}$ to $LiMn_2O_4$, thus, can be expressed as:

$$Li_4Mn_5O_{12} \xrightarrow{>700°C \text{ in } O_2} \alpha Li[Li_{1/3-\delta}Mn_{5/3+\delta}]O_4$$

$$+ \beta Li_2MnO_3 + \varepsilon O_2\uparrow. \quad [1]$$

Based on Eq. [1] and the point of view of electroneutrality, we deduced that $g_{Mn} = (5 + 3\delta)/6$, the mean oxidation state of manganese in the final products consisted of $\alpha Li[Li_{1/3-\delta}Mn_{5/3+\delta}]O_4 + \beta Li_2MnO_3$, $Z_{Mn} = (40 + 42\delta)/(10 + 15\delta)$, and the portion of Li_2MnO_3 (mol%) = $9\delta/(3\delta + 2)$. To verify the reaction of Eq. [1], the mean oxidation number of manganese (Z_{Mn}) in the samples synthesized at temperatures between 400 and 900°C was determined from the active oxygen content which was measured using the standard volumetric method of $KMnO_4$ titration. The measured Z_{Mn}, refined g_{Mn}, and the weight portion of Li_2MnO_3 (wt%) for these samples are plotted in Fig. 5 as a function of δ in $Li[Li_{1/3-\delta}Mn_{5/3+\delta}]O_4$, along with their calculated values based on the relations mentioned above.
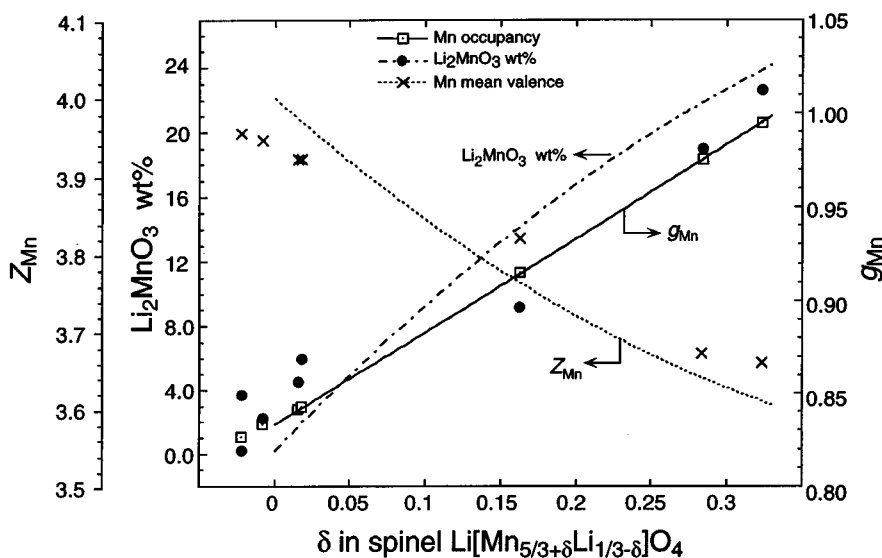
FIG. 5. Measured (marks) and calculated (lines) values of the mean valence of manganese, Z_{Mn}, refined site occupation factor of manganese in the $16d$ sites, g_{Mn}, and the portion of precipitated Li_2MnO_3, Li_2MnO_3 wt%, against δ in the spinel $Li[Li_{1/3-\delta}Mn_{5/3+\delta}]O_4$ for samples prepared at a temperature between 400 and 900°C.

Despite the insufficiency of the experimental data, good consistency is obtained in the trend of the changes of g_{Mn}, Li_2MnO_3 (wt%), and Z_{Mn} with δ in $Li[Li_{1/3-\delta}Mn_{5/3+\delta}]O_4$. Consequently, the composition of the spinel phase changes as the synthesis temperature is raised above 700°C, and it proceeds along the reaction of Eq. [1]. The value of δ in $Li[Li_{1/3-\delta}Mn_{5/3+\delta}]O_4$ changes from 0 to 1/3 when the synthesis temperature varies from 400 to 900°C. It is worth noting that the whole heating/cooling process for these samples proceeded rather slowly with 200 ml/min flow of pure O_2. The atmosphere has a significant effect on the final products; a complete decomposition of $Li_4Mn_5O_{12}$ to $LiMn_2O_4$ $+ Li_2MnO_3$ occurs at 580°C in nitrogen (7) but at temperatures above 900°C in oxygen. For verification, the data of Z_{Mn}, g_{Mn}, and Li_2MnO_3 (wt%) for $Li_4Mn_5O_{12}$ reheated at 580°C in nitrogen were also plotted in Fig. 5; these data points correspond to $\delta = 0.32$, which indicates a full decomposition of $Li_4Mn_5O_{12}$ to $2LiMn_2O_4 + Li_2MnO_3$.

Further verification of the formation of the pure phase spinel $Li[Li_{1/3-\delta}Mn_{5/3+\delta}]O_4$, or $Li[Li_xMn_{2-x}]O_4$ ($x = 1/3 - \delta$), is currently being done by varying the molar ratio Li/Mn in the starting materials. A good consistency in the Z_{Mn}, the g_{Mn}, and the ratio Li/Mn in the final products is obtained. Details of the crystal structure and the thermal stability of the spinel $Li[Li_xMn_{2-x}]O_4$ will be described separately.

4. CONCLUSION

Well-crystallized $Li_4Mn_5O_{12}$ has been prepared from the eutectic of LiOAc and $Mn(NO_3)_2$ under flowing oxygen.

Rietveld refinement of X-ray and neutron powder diffraction data indicated that $Li_4Mn_5O_{12}$ possesses a cubic spinel structure in which lithium ions occupy both the tetrahedral sites $8a$ and part of the octahedral sites $16d$, but not the $16c$ sites, while all the manganese ions occupy the $16d$ sites of space group $Fd\bar{3}m$. The lattice parameter was found to be sensitive to synthesis temperature as a result of the variation in manganese valence. The formation of the spinel $Li[Li_xMn_{2-x}]O_4$, in which x decreased from 1/3 to 0 as the synthesis temperature increased from 700 to 900°C, owing to the transition from Mn^{4+} to Mn^{3+} of a portion of the manganese ions, is elucidated with the concomitant formation of the minor phase Li_2MnO_3.

REFERENCES

1. J. M. Tarascon, W. R. McKinnon, F. Coowar, T. N. Bowmer, G. Amatucci, and D. Guyomard, *J. Electrochem. Soc.* **141**(6), 1421 (1994).
2. R. J. Gummow, A. de Kock, and M. M. Thackeray, *Solid State Ionics* **69**, 59 (1994).
3. M. M. Thackeray, M. F. Mansuetto, D. W. Dees, and D. R. Vissers, *Mater. Res. Bull.* **31**(2), 133 (1996).
4. D. Guyomard, J. M. Tarascon, *J. Electrochem. Soc.* **140**(11), 3071 (1993).

5. M. M. Thackeray, A. de Kock, M. H. Rossouw, D. Liles, R. Bittihn, and D. Hoge, *J. Electrochem. Soc.* **139**(2), 363 (1992).

6. T. Takada, H. Hayakawa, and E. Akiba, *J. Solid State Chem.* **115**, 420 (1995).

7. T. Takada, H. Hayakawa, T. Kumagai, and E. Akiba, *J. Solid State Chem.* **121**, 79 (1996).

8. M. N. Richard, E. W. Fuller, and J. R. Dahn, *Solid State Ionics* **73**, 81 (1994).

9. M. M. Thackeray, A. de Kock, and W. I. F. David, *Mater. Res. Bull.* **28**, 1041 (1993).

10. A. de Kock, M. H. Rossouw, L. A. Picciotto, M. M. Thackeray, W. I. F. David, R. M. Ibberson, *Mater. Res. Bull.* **25**, 657 (1990).

11. A. Yamada, *J. Solid State Chem.* **122**, 160 (1996).

12. R. A. Young, "The Rietveld Method," Oxford Univ. Press, New York, 1993.

13. F. Izumi, *in* "The Rietveld Method" (R. A. Young, Ed.), pp. 236–253. Oxford Univ. Press, New York, 1993.

14. Japan Industrial Standard (JIS) M8233-1982 "Determination of Active Oxygen Content in Manganese Ores."

15. P. Strobel and B. Lambert-Andron, *J. Solid State Chem.* **75**, 90 (1988).

16. G. Blasse, *Philips Res. Rep.*, *Suppl.* **3**, 122 (1964).

17. J. B. Goodenough and A. L. Lobe, *Phys. Rev.* **98**, 391 (1955).

18. B. K. Vainshtein, V. M. Fridkin, and V. L. Indenbom, "Structure of Crystal," pp. 71–80, Springer-Verlag, Berlin, 1995.

.